

Variational Gibbs State Preparation on NISQ devices

Mirko Consiglio¹, Jacopo Settimo^{2,3,4}, Andrea Giordano⁴, Carlo Mastroianni⁴, Francesco Plastina^{2,3}, Salvatore Lorenzo⁵, Sabrina Maniscalco^{6,7}, John Gool⁸, and Tony J. G. Apollaro¹

¹Department of Physics, University of Malta, Msida MSD 2080, Malta

²Dipartimento di Fisica, Università della Calabria, 87036 Arcavacata di Rende (CS), Italy

³INFN, gruppo collegato di Cosenza, 87036 Arcavacata di Rende (CS), Italy

⁴ICAR-CNR, 87036 Rende (CS), Italy

⁵Università degli Studi di Palermo, Dipartimento di Fisica e Chimica - Emilio Segrè, via Archirafi 36, I-90123 Palermo, Italy

⁶QTF Centre of Excellence, Department of Physics, University of Helsinki, P.O. Box 43, FI-00014 Helsinki, Finland

⁷Algorithmiq Ltd, Kanavakatu 3 C, FI-00160 Helsinki, Finland

⁸School of Physics, Trinity College Dublin, College Green, Dublin 2, Ireland

The preparation of an equilibrium thermal state of a quantum many-body system on noisy intermediate-scale quantum (NISQ) devices is an important task in order to extend the range of applications of quantum computation. Faithful Gibbs state preparation would pave the way to investigate protocols such as thermalization and out-of-equilibrium thermodynamics, as well as providing useful resources for quantum algorithms, where sampling from Gibbs states constitutes a key subroutine. We propose a variational quantum algorithm (VQA) to prepare Gibbs states of a quantum many-body system. The novelty of our VQA consists in implementing a parameterized quantum circuit acting on two distinct, yet connected, quantum registers. The VQA evaluates the Helmholtz free energy, where the von Neumann entropy is obtained via post-processing of computational basis measurements on one register, while the Gibbs state is prepared on the other register, via a unitary rotation in the energy basis. Finally, we benchmark our VQA by preparing Gibbs states of the transverse field Ising model and achieve remarkably high fidelities across a broad range of temperatures in statevector simulations. We also assess the performance of the VQA on IBM quantum computers, showcasing its feasibility on current NISQ devices.

1 Introduction

An integral task in quantum state preparation is the generation of finite-temperature thermal states of a given Hamiltonian, on a quantum computer. Indeed, Gibbs states (also known as thermal states) can be used for quantum simulation [1], quantum machine learning [2, 3], quantum optimization [4], and the

study of open quantum systems [5]. In particular, combinatorial optimization problems [4], semi-definite programming [6], and training of quantum Boltzmann machines [2], can be tackled by sampling from well-prepared Gibbs states.

The preparation of an arbitrary initial state is a challenging task in general, with finding the ground-state of a Hamiltonian being a *QMA*-hard problem [7]. Preparing Gibbs states, specifically at low temperatures, could be as hard as finding the ground-state of that Hamiltonian [8]. The first algorithms for preparing Gibbs states were based on the idea of coupling the system to a register of ancillary qubits, and letting the system and environment evolve under a joint Hamiltonian, simulating the physical process of thermalization, such as in Refs. [5, 9, 10], while others relied on dimension reduction [11].

The algorithm proposed in this manuscript, for preparing Gibbs states, can be placed in the category of variational quantum algorithms (VQAs), such as in Refs. [12–16], and similarly for preparing thermal double (TFD) states [17–19]. Variational ansätze based on multi-scale entanglement renormalization [20] and product spectrum ansatz [21] have also been proposed in order to prepare Gibbs states.

Alternative algorithms prepare thermal states through quantum imaginary time evolution, such as in Refs. [22–26], starting from a maximally mixed state, while others start from a maximally entangled state [27]. Ref. [28] proposed quantum-assisted simulation to prepare thermal states, which does not require a hybrid quantum-classical feedback loop. In addition, methods exist to sample Gibbs state expectation values, rather than prepare the Gibbs state directly, such as in quantum metropolis methods [29, 30], imaginary time evolution applied to pure states [31], and random quantum circuits using intermediate measurements [32].

Recent methods also propose using rounding promises [33], fluctuation theorems [34], pure thermal shadow tomography [35], and minimally entan-

Mirko Consiglio: mirko.consiglio@um.edu.mt

gled typical thermal states for finite temperature simulations [36].

The goal of this work is to propose a VQA that efficiently prepares Gibbs states on noisy intermediate-scale quantum (NISQ) computers, employing the free energy as a (physically-motivated) objective function. This requires the evaluation of the von Neumann entropy [37], which is generally hard to obtain from a quantum register. In contrast to some of the currently employed VQAs [10, 12–15, 17, 19, 32], which employ truncated equations to approximate it, we directly estimate the von Neumann entropy, without any truncation and with an error solely dependent on the number of shots, using sufficiently expressible ansätze capable of preparing the Boltzmann distribution. Our VQA, in fact, is composed of two ansätze: a heuristic, shallow one that prepares the Boltzmann distribution, for a given temperature; and another one, possibly designed with a problem-inspired approach, which depends on the Hamiltonian, while being independent of the temperature.

The paper is organized as follows: in Section 2, we present the VQA for preparing Gibbs states, as well as briefly mentioning the error analysis of the algorithm along with the parameterized quantum circuit (PQC), with further details found in Appendices A and B; in Section 3, we apply the algorithm to the Ising model, using both statevector and noisy simulations, as well as running the algorithm on IBM quantum hardware; and finally, in Section 4, we draw our conclusions and discuss future prospects of this work.

2 Variational Gibbs State Preparation

Let's consider a Hamiltonian \mathcal{H} , describing n interacting qubits. Then, the Gibbs state at inverse temperature $\beta \equiv 1/k_B T$, where k_B Boltzmann constant and T is the temperature, is defined as

$$\rho_\beta = \frac{e^{-\beta\mathcal{H}}}{\mathcal{Z}_\beta}, \quad (1)$$

where the partition function \mathcal{Z}_β is

$$\mathcal{Z}_\beta = \text{Tr}\{e^{-\beta\mathcal{H}}\} = \sum_{i=0}^{d-1} e^{-\beta E_i}. \quad (2)$$

Here $d = 2^n$, while $\{E_i\}$ are the eigenenergies of \mathcal{H} (with $\{|E_i\rangle\}$ denoting the corresponding eigenstates), i.e. $\mathcal{H}|E_i\rangle = E_i|E_i\rangle$.

For a general state ρ , one can define a generalized Helmholtz free energy as

$$\mathcal{F}_\beta(\rho) = \text{Tr}\{\mathcal{H}\rho\} - \beta^{-1}\mathcal{S}(\rho), \quad (3)$$

where the von Neumann entropy $\mathcal{S}(\rho)$ can be expressed in terms of the eigenvalues, p_i , of ρ ,

$$\mathcal{S}(\rho) = -\sum_{i=0}^{d-1} p_i \ln p_i. \quad (4)$$

Since the Gibbs state is the unique state that minimizes the free energy of \mathcal{H} [38], a variational procedure can be put forward that takes Eq. (3) as an objective function, such that

$$\rho_\beta = \arg \min_{\rho} \mathcal{F}_\beta(\rho). \quad (5)$$

In this case, $p_i = \exp(-\beta E_i)/\mathcal{Z}_\beta$ is the probability of getting the eigenstate $|E_i\rangle$ from the ensemble ρ_β .

2.1 Framework of the Algorithm

The difficulty in measuring the von Neumann entropy, defined by Eq. (4), of a quantum state on a NISQ device is usually the challenging part of variational Gibbs state preparation algorithms, as $\mathcal{S}(\rho)$ is not an observable. With this in mind, we present a VQA that avoids the direct measurement of the von Neumann entropy on a quantum computer, by using a carefully constructed PQC.

When preparing an n -qubit state, given that a quantum computer operates using only unitary gates, starting from the register input state $|0\rangle^{\otimes n}$, the final quantum state of the entire register will be pure. As a result, in order to prepare an n -qubit Gibbs state on the system register, we require an $m \leq n$ -qubit ancillary register. For example, in the case of the infinite-temperature Gibbs state, which is a fully mixed state, we require $m = n$ qubits in the ancillary register to achieve maximal von Neumann entropy. In order to evaluate the von Neumann entropy, without any truncation, we need to prepare the entire Boltzmann distribution on the ancillary register, hence, we set $m = n$, irrespective of the temperature.

We shall denote the ancillary register as A , while the preparation of the Gibbs state will be carried out on the system register S . The purpose of the VQA is to effectively create the Boltzmann distribution on A , which is then imposed on S , via intermediary CNOT gates, to generate a diagonal mixed state. In the ancillary register we can choose a unitary ansatz capable of preparing such a probability distribution. Thus, the ancillary qubits are responsible for classically mixing in the probabilities of the thermal state, while also being able to access these probabilities via measurements in the computational basis. On the other hand, the system register will host the preparation of the Gibbs state as well as the measurement of the expectation value of our desired Hamiltonian.

The specific design of the PQC instead allows classical post-processing of simple measurement results, carried out on ancillary qubits in the computational basis, to determine the von Neumann entropy. A diagrammatic representation of the structure of the PQC is shown in Fig. 1. Note that while the PQC of the algorithm has to have a particular structure — a unitary acting on the ancillae and a unitary acting on the system, connected by intermediary CNOT gates — it is not dependent on the choice of Hamiltonian \mathcal{H} ,

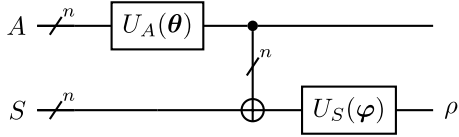


Figure 1: PQC for Gibbs state preparation, with systems A and S each carrying n qubits. CNOT gates act between each qubit A_i and corresponding S_i .

inverse temperature β , or the variational ansätze, U_A and U_S , employed within. This is in addition to enjoying a sub-exponential scaling in the number of shots needed to precisely compute the Boltzmann probabilities. A qualitative analysis of a power-law scaling is presented in Appendix A.

2.2 Modular Structure of the PQC

The PQC, as shown in Fig. 1 for the VQA, is composed of a unitary gate U_A acting on the ancillary qubits, and a unitary gate U_S acting on the system qubits, with CNOT gates in between. Note that the circuit notation we are using here means that there are n qubits for both the system and the ancillae, as well as n CNOT gates that act in parallel, and are denoted as

$$\text{CNOT}_{AS} \equiv \bigotimes_{i=0}^{n-1} \text{CNOT}_{A_i S_i}. \quad (6)$$

The parameterized unitary U_A acting on the ancillae, followed by CNOT gates between the ancillary and system qubits, is responsible for preparing a probability distribution on the system. The parameterized unitary U_S is then applied on the system qubits to transform the computational basis states into the eigenstates of the Hamiltonian.

A general unitary gate of dimension $d = 2^n$ is given by

$$U_A = \begin{pmatrix} u_{0,0} & u_{0,1} & \cdots & u_{0,d-1} \\ u_{1,0} & u_{1,1} & \cdots & u_{1,d-1} \\ \vdots & \vdots & \ddots & \vdots \\ u_{d-1,0} & u_{d-1,1} & \cdots & u_{d-1,d-1} \end{pmatrix}. \quad (7)$$

Starting with the initial state of the $2n$ -qubit register, $|0\rangle_{AS}^{\otimes 2n}$, we apply the unitary gate U_A on the ancillae to get a quantum state $|\psi\rangle_A$, such that

$$(U_A \otimes I_S) |0\rangle_{AS}^{\otimes 2n} = |\psi\rangle_A \otimes |0\rangle_S^{\otimes n}, \quad (8)$$

where

$$|\psi\rangle_A = \sum_{i=0}^{d-1} u_{i,0} |i\rangle_A, \quad (9)$$

and I_S is the identity acting on the system. The next step is to prepare a classical probability mixture on the system qubits, which can be done by applying

CNOT gates between each ancilla and system qubit. This results in a state

$$\text{CNOT}_{AS} \left(|\psi\rangle_A \otimes |0\rangle_S^{\otimes n} \right) = \sum_{i=0}^{d-1} u_{i,0} |i\rangle_A \otimes |i\rangle_S. \quad (10)$$

By then tracing out the ancillary qubits, we arrive at

$$\begin{aligned} & \text{Tr}_A \left\{ \text{CNOT}_{AS} (|\psi\rangle\langle\psi|_A \otimes |0\rangle\langle 0|_S^{\otimes n}) \text{CNOT}_{AS}^\dagger \right\} \\ &= \text{diag} (|u_{0,0}|^2, |u_{1,0}|^2, \dots, |u_{d-1,0}|^2) \\ &= \text{diag} (p_0, p_1, \dots, p_{d-1}), \end{aligned} \quad (11)$$

ending up with a diagonal mixed state on the system, with probabilities given directly by the absolute square of the entries of the first column of U_A , that is, $p_i = |u_{i,0}|^2$. If the system qubits were traced out instead, we would end up with the same diagonal mixed state,

$$\begin{aligned} & \text{Tr}_S \left\{ \text{CNOT}_{AS} (|\psi\rangle\langle\psi|_A \otimes |0\rangle\langle 0|_S^{\otimes n}) \text{CNOT}_{AS}^\dagger \right\} \\ &= \text{diag} (|u_{0,0}|^2, |u_{1,0}|^2, \dots, |u_{d-1,0}|^2) \\ &= \text{diag} (p_0, p_1, \dots, p_{d-1}), \end{aligned} \quad (12)$$

This implies that by measuring in the computational basis of the ancillary qubits, we can determine the probabilities p_i , which can then be post-processed to determine the von Neumann entropy \mathcal{S} of the state ρ via Eq. (4) (since the entropy of A is the same as that of S). As a result, since U_A only serves to create a probability distribution from the entries of the first column, we can do away with a parameterized orthogonal (real unitary) operator, thus requiring less gates and parameters for the ancillary ansatz.

The unitary gate U_S then serves to transform the computational basis states of the system qubits to the eigenstates of the Gibbs state, such that

$$\begin{aligned} \rho &= U_S \text{diag} (p_0, p_1, \dots, p_{d-1}) U_S^\dagger \\ &= \sum_{i=0}^{d-1} p_i |\psi_i\rangle\langle\psi_i|, \end{aligned} \quad (13)$$

where the expectation value $\text{Tr}\{\mathcal{H}\rho\}$ of the Hamiltonian can be measured. Ideally, at the end of the optimization procedure, $p_i = \exp(-\beta E_i) / \mathcal{Z}_\beta$ and $|\psi_i\rangle = |E_i\rangle$, so that we get

$$\rho_\beta = \sum_{i=0}^{d-1} \frac{e^{-\beta E_i}}{\mathcal{Z}_\beta} |E_i\rangle\langle E_i|. \quad (14)$$

The VQA therefore avoids the entire difficulty of measuring the von Neumann entropy of a mixed state on a quantum computer, and instead transfers the task of post-processing measurement results to the classical computer, which is much more tractable.

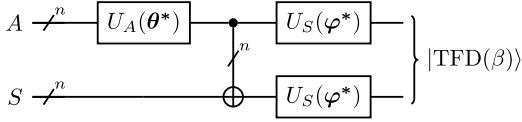


Figure 2: Optimal PQC for TFD state preparation, with systems A and S each carrying n qubits. CNOT gates act between each qubit A_i and corresponding S_i .

2.3 Objective Function

Finally, we can define the objective function of our VQA to minimize the free energy (3), via our constructed PQC, to obtain the Gibbs state

$$\begin{aligned} \rho_\beta &= \arg \min_{\theta, \varphi} \mathcal{F}_\beta(\rho(\theta, \varphi)) \\ &= \arg \min_{\theta, \varphi} (\text{Tr}\{\mathcal{H}\rho_S(\theta, \varphi)\} - \beta^{-1} \mathcal{S}(\rho_A(\theta))). \end{aligned} \quad (15)$$

It is noteworthy to mention that while the energy expectation depends on both sets of angles θ (as U_A is responsible for parameterizing the Boltzmann distribution) and φ (as U_S is responsible for parameterizing the eigenstates of the Gibbs state), the calculation of the von Neumann entropy only depends on θ .

Furthermore, once we obtain the optimal parameters θ^* , φ^* , preparing the Gibbs state ρ_β on the system qubits S , one can place the same unitary U_S with optimal parameters φ^* on the ancillary qubits to prepare the TFD state on the entire qubit register, as shown in Fig. 2. A TFD state [12, 17, 19] is defined as

$$|\text{TFD}(\beta)\rangle = \sum_{i=0}^{d-1} \frac{e^{-\frac{\beta E_i}{2}}}{\sqrt{\mathcal{Z}_\beta}} |i\rangle_A \otimes |i\rangle_S. \quad (16)$$

Notice that this is equivalent to Eq. (10) after applying U_S on both registers. Tracing out either the ancilla or system register yields the same Gibbs state on the other register.

$$R_P(\varphi_i, \varphi_j) = R_{YX}(\varphi_j) \cdot R_{XY}(\varphi_i) = \begin{pmatrix} \cos\left(\frac{\varphi_i + \varphi_j}{2}\right) & 0 & 0 & \sin\left(\frac{\varphi_i + \varphi_j}{2}\right) \\ 0 & \cos\left(\frac{\varphi_i - \varphi_j}{2}\right) & -\sin\left(\frac{\varphi_i - \varphi_j}{2}\right) & 0 \\ 0 & \sin\left(\frac{\varphi_i - \varphi_j}{2}\right) & \cos\left(\frac{\varphi_i - \varphi_j}{2}\right) & 0 \\ -\sin\left(\frac{\varphi_i + \varphi_j}{2}\right) & 0 & 0 & \cos\left(\frac{\varphi_i + \varphi_j}{2}\right) \end{pmatrix}, \quad (18)$$

which can be decomposed into two CNOT gates and

3 Performance of the VQA

In this Section we assess the performance of the VQA for Gibbs state preparation of an Ising model. The Ising model is defined as

$$\mathcal{H} = - \sum_{i=1}^n \sigma_i^x \sigma_{i+1}^x - h \sum_{i=1}^n \sigma_i^z. \quad (17)$$

The Ising Hamiltonian is a well-known model [39], and here we only report one relevant property for implementing a problem-inspired ansatz for U_S . The Hamiltonian in Eq. (17) commutes with the parity operator $\mathcal{P} = \prod_{i=0}^{n-1} \sigma_i^z$. As a consequence, the eigenstates of \mathcal{H} have definite parity, and so will the eigenstates of ρ_β .

We use the Uhlmann-Josza fidelity [40], defined as $F(\rho_1, \rho_2) = (\text{Tr}\{\sqrt{\sqrt{\rho_2}\rho_1\sqrt{\rho_2}}\})^2$, as a figure of merit for the performance of our VQA, since it describes how “close” the prepared state is to the Gibbs state, and is also the most commonly-employed measure of distinguishability. However, other measures can be used, which have different interpretations. One example is the trace distance [41], which enjoys the property that, if its value between the two states is bounded by ϵ , expectation values computed on the effectively prepared state, differ from those taken on the Gibbs state by an amount that is, at most, proportional to ϵ [34]. Another choice is the relative entropy [41], which describes the distinguishability between the two states as the surprise that occurs when an event happens that is not possible with the true Gibbs state [42].

We use a simple, linearly entangled PQC for the unitary U_A , with parameterized $R_Y(\theta_i)$ gates, and CNOTs as the entangling gates. This ansatz is hardware efficient and is sufficient to produce real amplitudes for preparing the probability distribution. Note that we require the use of entangling gates, as otherwise we will not be able to prepare any arbitrary probability distribution, including the Boltzmann distribution of the Ising model. A proof of this is given in Appendix B.

For the unitary U_S , we choose a parity-preserving PQC. We employ a brick-wall structure, with the gates being $R_{XY}(\varphi_i)$ followed by $R_{YX}(\varphi_j)$ gates. If we combine the two gates, which we denote as $R_P(\varphi_i, \varphi_j)$, we get

six \sqrt{X} gates. One layer of the unitary acting on the

# of parameters	$n(l_A + 1) + 2nl_S$	$\mathcal{O}(n(l_A + l_S))$
# of CNOT gates	$(n - 1)l_A + 2nl_S + n$	$\mathcal{O}(n(l_A + l_S))$
# of \sqrt{X} gates	$2n(l_A + 1) + 6nl_S$	$\mathcal{O}(n(l_A + l_S))$
Circuit depth	$(n + 1)l_A + Pl_S + 3$	$\mathcal{O}(nl_A + l_S)$

Table 1: Scaling of the VQA assuming a closed ladder connectivity, for $n > 2$, where l_A and l_S are the number of ancilla ansatz and system ansatz layers, respectively, and P is 12 when n is even and 18 when n is odd.

# of parameters	$2n^2$	$\mathcal{O}(n^2)$
# of CNOT gates	$2n^2 - 1$	$\mathcal{O}(n^2)$
# of \sqrt{X} gates	$2n(3n - 2)$	$\mathcal{O}(n^2)$
Circuit depth	$(P + 1)n - P + 4$	$\mathcal{O}(n)$

Table 2: Scaling of the VQA assuming a closed ladder connectivity, for $n > 2$, with $l_A = 1$, and $l_S = n - 1$, and P is 12 when n is even and 18 when n is odd. The depth counts both CNOT and \sqrt{X} gates.

system qubits consists of a brick-wall structure, composed of an even-odd sublayer of R_P gates, followed by an odd-even sublayer of R_P gates. Table 1 shows the scaling of the VQA assuming a closed ladder connectivity, for $n > 2$. An example of a PQC, split into a four-qubit ancilla register, and a four-qubit system register, is shown in Fig. 3.

3.1 Statevector Results

Fig. 4 show the fidelity of the generated mixed state when compared with the exact Gibbs state of the Ising model with $h = 0.5, 1.0, 1.5$, respectively, across a range of temperatures for system size between two to six qubits. The VQA was carried out using statevector simulations with the Broyden–Fletcher–Goldfarb–Shanno (BFGS) optimizer [43]. We used one layer for the ancilla ansatz, and $n - 1$ layers for the system ansatz, with the scaling highlighted in Table 2. The number of layers was heuristically chosen to satisfy, at most, a polynomial scaling in quantum resources, while achieving a fidelity higher than 95% in statevector simulations. Furthermore, in order to alleviate the issue of getting stuck in local minima, the optimizer is embedded in a Monte Carlo framework, that is, taking multiple random initial positions and carrying out a local optimization from each position — which we call a ‘run’ — and finally taking the global minimum to be the minimum over all runs.

A total of 100 runs of BFGS per β were carried out to verify the reachability of the PQC, with Fig. 4 showcasing the maximal fidelity achieved for each β out of all runs. The results show that, indeed, our VQA, is able to reach a very high fidelity $F \gtrsim 98\%$ for up to six-qubit Gibbs states of the Ising model. In the case of the extremal points, that is $\beta \rightarrow 0$ and $\beta \rightarrow \infty$, the fidelity reaches unity, for all investigated system sizes. On the other hand, for intermediary

# of iterations for each run	$100n$	$\mathcal{O}(n)$
# of function evaluations for each run	$200n$	$\mathcal{O}(n)$
# of circuits per function evaluation	2	$\mathcal{O}(1)$
# of circuit evaluations for each run	$400n$	$\mathcal{O}(n)$
# of shots for each circuit evaluation	1024	$\mathcal{O}(1)$

Table 3: Scaling of SPSA for noisy simulations and on quantum hardware.

temperatures $\beta \sim 1$, the fidelity decreases with the number of qubits, which could be attributed to one layer of U_A not being expressible enough to prepare the Boltzmann distribution around intermediary temperatures (since the von Neumann entropy depends solely on $U_A(\theta)$ as in Eq. (15)).

3.2 Noisy Simulation Results

The next step was to carry out noisy simulations of the VQA. We took the noise model of `ibmq_guadalupe` [44] for the Ising model with $h = 0.5$, similarly with one layer for the ancilla ansatz and $n - 1$ layers for the system ansatz. However, it must be noted that in this case, the scaling of the algorithm does not follow Table 2, due to the fact that `ibmq_guadalupe` does not have a closed ladder connectivity. As a result, transpilation was carried out by the Qiskit transpiler using the SABRE algorithm [45]. Apart from this, due to the BFGS optimizer being incapable of optimizing a noisy objective function, an optimizer that accommodates noisy measurements was chosen: simultaneous perturbation stochastic approximation (SPSA) [46].

Using SPSA, ten runs were carried out for each β , while the number of iterations was taken to be $100n$ for each run, with only two measurements at each iteration to estimate the gradient, i.e. $200n$. As a consequence, a total of $2000n$ function evaluations were used to obtain the fidelity for each β shown in Fig. 5 (with an extra 50 function evaluations at each run to calibrate the hyperparameters of SPSA). Similar to the number of layers, the choice of the number of iterations was heuristically chosen so that, at most, the scaling is linear, while still retaining a fidelity greater than 95% for the two- and three-qubit noisy simulation cases.

To measure the energy expectation value of the Ising model $\text{Tr}\{\mathcal{H}\rho\}$, we need to split the Ising Hamiltonian into its constituent Pauli strings, whose number scales linearly with the number of qubits as $2n$. However, we can group the $\sigma^x\sigma^x$ terms, as well as the σ^z terms, and measure them simultaneously, reducing the number of measurement circuits to two. Each circuit was also measured with 1024 shots. The M3 package [47] was also utilized to perform basic error mitigation. A summary of the optimization scaling is shown in Table 3.

From Fig. 5, one can see that the fidelity is signifi-

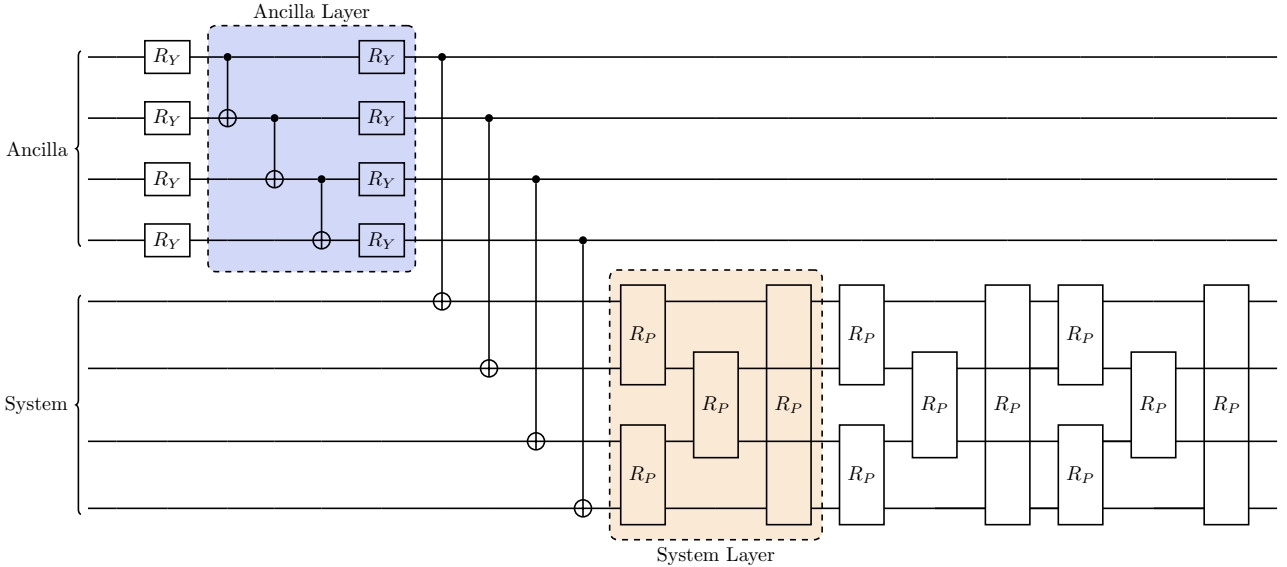


Figure 3: Example of an eight-qubit PQC, consisting of one ancilla layer acting on a four-qubit register, and three $(n - 1)$ system layers acting on another four-qubit register. Each R_Y gate is parameterized with one parameter θ_i , while each R_P gate has two parameters φ_i and φ_j . The R_P gate is defined in Eq. (18). Note that the intermediary CNOT gates, as well as the R_P gates acting on qubits two and three, and on qubits one and four of the system, can be carried out in parallel, respectively.

cantly high in the case of $n = 2, 3, 4$. However, in the case of $n = 5, 6$, the Gibbs state is only faithfully prepared for low β . This can be attributed to the level of noise present in the optimization procedure, with the transpiled circuits going well beyond the quantum volume of `ibmq_guadalupe`. There are also some points which obtain a fidelity worse for five qubits than six qubits, which could be due to the larger depth acquired by an odd number of qubits in the system ansatz, as highlighted in Table 2.

3.3 IBM Quantum Device Results

Finally, the VQA was carried out on an actual quantum device. Fig. 6 displays the fidelity of Gibbs states obtained by running on IBM quantum hardware [44], specifically `ibmq_nairobi`. Similarly to the noisy simulations, SPSA was used; however, this time, with only one run for each β in the case $n = 2$, and two runs in the case $n = 3$, with $100n$ iterations and 1024 shots. The Gibbs states were obtained by taking the optimal parameters from the optimization carried out on `ibmq_nairobi`, and determining the statevector on a classical computer.

The solid lines in Fig. 6 represent the two- and three-qubit results. At all points, the two-qubit Gibbs state shows excellent fidelity. On the other hand, the three-qubit Gibbs state is remarkably reproduced at certain temperatures, while it is lacking at other points. Since `ibmq_nairobi` does not have a closed ladder connectivity, several SWAP gates are necessary for carrying out transpilation. To reduce the number of SWAP gates, we carried out another run

at each β , where we removed the R_P gate acting on non-adjacent qubits in the system layers, with the result shown in the dashed line of Fig. 6. A considerable improvement in fidelity is achieved at the points where fidelity was lacking in the previous case. Since the available running time on the quantum device was limited, the amount of runs is still too low to determine the reason as to why the Gibbs state was not achieved with a decent fidelity. Nevertheless, comparing the results of Fig. 6, with the statevector results in Fig. 4 and with the noise-simulated results in Fig. 5, we conclude that limited connectivity, combined with device noise, is severely hampering the effectiveness of the VQA.

In addition, quantum state tomography for the two-qubit case was carried out on `ibmq_nairobi`, with 1024 shots, for the cases of $\beta = 0, 1, 5$, where the fidelities obtained were 0.992, 0.979, and 0.907, respectively. A 3D bar plot of the tomographic results can be seen in the right column Fig. 7, and compared with the analytical form of the Gibbs state on the left column. The largest discrepancies can be witnessed in the off-diagonal terms, which increase as β increases, as well as showcasing symptoms of amplitude damping. This could be attributed to the thermal relaxation and dephasing noise present in the quantum devices, leading to an overall decoherence in the Gibbs state.

While noisy simulations were ran using the calibration data of `ibmq_guadalupe` — since it has access of up to 16 qubits — the actual hardware used for the two- and three-qubit Gibbs state preparation was `ibmq_nairobi`, due to its accessibility.

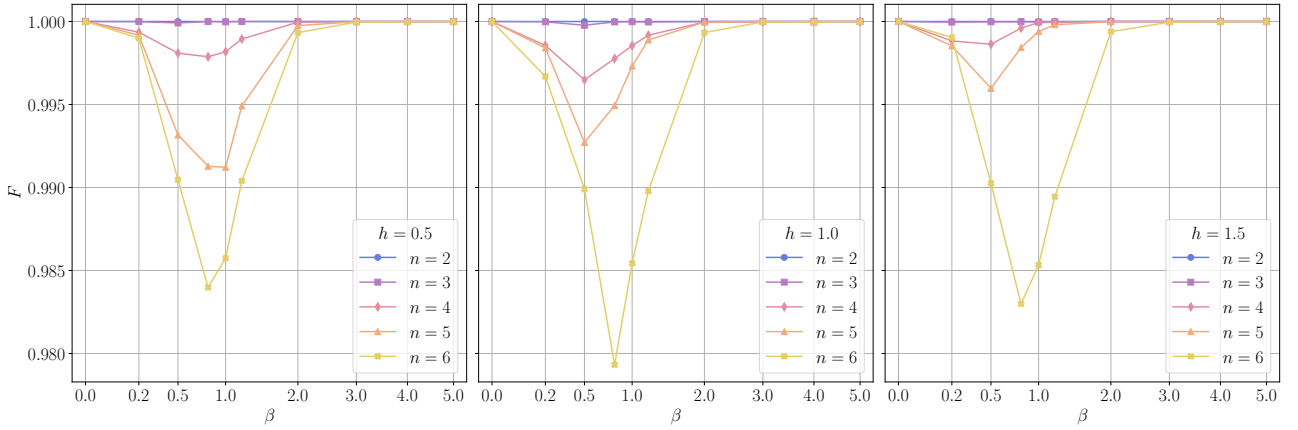


Figure 4: Fidelity F , of the obtained state via statevector simulations (using BFGS) with the exact Gibbs state, vs inverse temperature β , for two to six qubits of the Ising model with $h = 0.5, 1.0, 1.5$. A total of 100 runs are made for each point, with the optimal state taken to be the one that maximizes the fidelity.

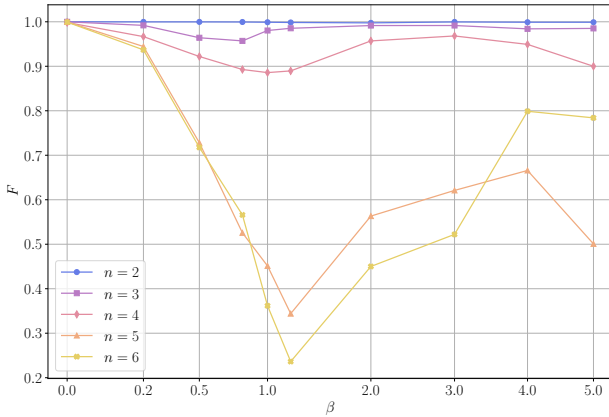


Figure 5: Fidelity F , of the obtained state via noisy simulations (using SPSA) of `ibmq_guadalupe` with the exact Gibbs state, vs inverse temperature β , for two to six qubits of the Ising model with $h = 0.5$. A total of ten runs are made for each point, with the optimal state taken to be the one that maximizes the fidelity.

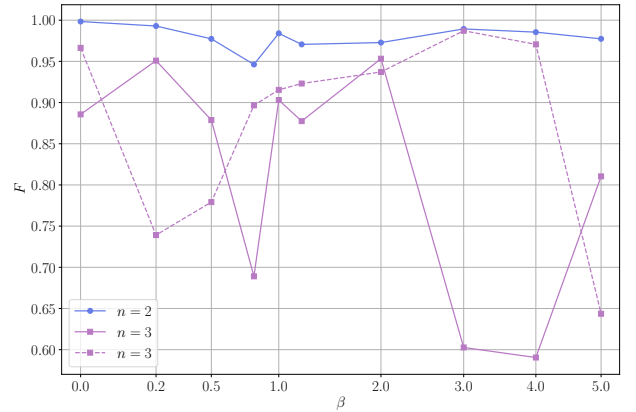


Figure 6: Fidelity F , of the obtained state (using SPSA) running directly on `ibmq_nairobi` with the exact Gibbs state, vs inverse temperature β , for two and three qubits of the Ising model with $h = 0.5$. The dashed line represents the run with no R_P gate between non-adjacent qubits in the system layers. One run is carried out for $n = 2$, and $n = 3$ for the dashed line, and two runs for $n = 3$ for the solid line.

4 Conclusion

We addressed the preparation of a thermal equilibrium state of a quantum many-body system on a NISQ device. We exploited the uniqueness of the Gibbs state as the state that minimizes the Helmholtz free energy, thus providing a faithful objective function for a VQA.

The novelty of the proposed VQA consisted in splitting the PQC in two parameterized unitaries, one acting on an ancillary register, and one on a system register. The former is tasked with determining the Boltzmann weights of the Gibbs distribution, corresponding to a given temperature, while the latter performs the rotation from the computational basis to the energy basis of a given Hamiltonian.

We benchmarked our VQA preparing the Gibbs state of the transverse field Ising model and ob-

tained fidelities $F \simeq 1$ for system sizes up to six qubits in statevector simulations, across a broad range of temperatures, with a slight dip at intermediate ones. However, performance on current NISQ devices, investigated both by noisy simulations and real-hardware execution on IBM devices, showed a degradation in the results of the VQA with increasing system size. This may have been caused by the limited connectivity and the noise present in the device. Nevertheless, executing our VQA on NISQ devices still provides an improvement upon the recent developments in variational Gibbs state preparation, see e.g., Ref. [19].

As a final remark, we notice that the structure of our VQA does not depend on the specific Hamiltonian to be tackled, nor on any prior knowledge of its spectrum. For example, the structure of the unitary

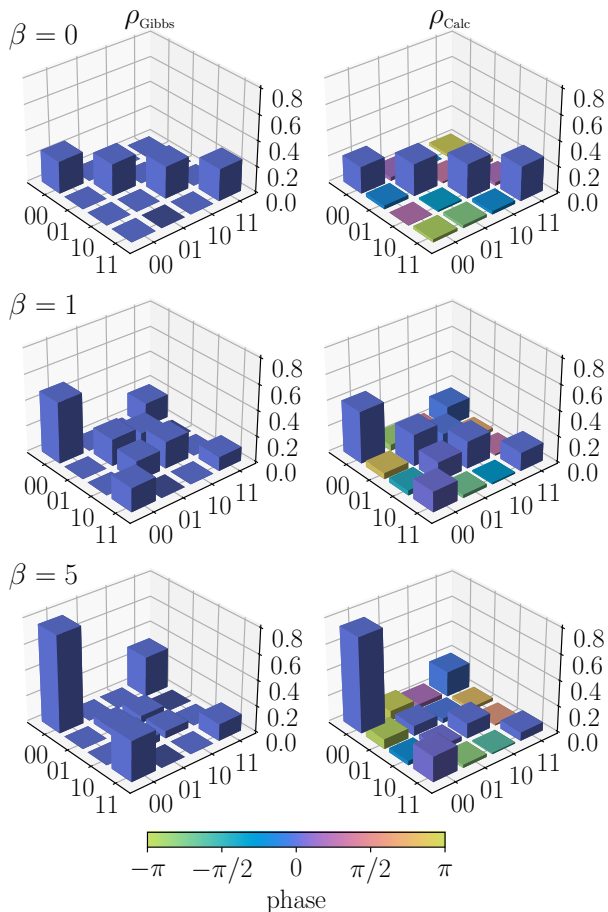


Figure 7: 3D bar plot of the two qubit results from `ibm_nairobi` for $\beta = 0, 1, 5$, of the Ising model with $h = 0.5$. The analytical Gibbs states are shown in the left column, while the tomographically obtained Gibbs States are shown in the right column.

$U_S(\varphi)$ could be adjusted in order to match some specific features of the eigenstates (if these are known), or the parameterized unitary $U_A(\theta)$ could be replaced by a deterministic procedure (e.g., the one reported in [48]), if the probabilities of the Boltzmann distribution are known.

However, even without requiring any such knowledge, our ‘Hamiltonian-agnostic’ variational approach gives an effective way to prepare Gibbs states of arbitrary quantum many-body systems on a quantum computer, providing an advancement over previous methods, especially thanks to the modular structure of our PQC. This could significantly contribute to both performing quantum thermodynamical experiments on a quantum computer, as well as faithfully preparing Gibbs states to be used in a great variety of computational tasks.

The Python code for running the statevector simulations, using Qulacs [49], and the noisy simulations, as well as the Runtime Program, using Qiskit [50], can be found on GitHub [51].

Acknowledgments

M.C. acknowledges fruitful discussions with Jake Xuereb and Felix Binder on the thermodynamical concepts of the manuscript. M.C. and T.J.G.A. would like to also thank Matteo Rossi, Marco Cattaneo and Zoe Holmes for the interesting discussions on the algorithmic component of the Manuscript. M.C. acknowledges funding by TESS (Tertiary Education Scholarships Scheme), and project QVAQT (Quantum variational algorithms for quantum technologies) REP-2022-003 financed by the Malta Council for Science & Technology, for and on behalf of the Foundation for Science and Technology, through the FUSION: R&I Research Excellence Programme. J.G. is funded by a Science Foundation Ireland-Royal Society University Research Fellowship and his work is also supported by the European Research Council Starting Grant ODYSSEY (Grant Agreement No. 758403). We acknowledge the use of IBM Quantum services for this work; the views expressed are those of the authors, and do not reflect the official policy or position of IBM or the IBM Quantum team.

References

- [1] Andrew M. Childs, Dmitri Maslov, Yunseong Nam, Neil J. Ross, and Yuan Su. “Toward the first quantum simulation with quantum speedup”. *Proceedings of the National Academy of Sciences* **115**, 9456–9461 (2018).
- [2] Mária Kieferová and Nathan Wiebe. “Tomography and generative training with quantum Boltzmann machines”. *Phys. Rev. A* **96**, 062327 (2017).
- [3] Jacob Biamonte, Peter Wittek, Nicola Pancotti, Patrick Rebentrost, Nathan Wiebe, and Seth Lloyd. “Quantum machine learning”. *Nature* **549**, 195–202 (2017).
- [4] R. D. Somma, S. Boixo, H. Barnum, and E. Knill. “Quantum Simulations of Classical Annealing Processes”. *Phys. Rev. Lett.* **101**, 130504 (2008).
- [5] David Poulin and Pawel Wocjan. “Sampling from the Thermal Quantum Gibbs State and Evaluating Partition Functions with a Quantum Computer”. *Phys. Rev. Lett.* **103**, 220502 (2009).
- [6] Fernando G. S. L. Brandao and Krysta Svore. “Quantum Speed-ups for Semidefinite Programming” (2016).
- [7] John Watrous. “Quantum Computational Complexity” (2008).
- [8] Dorit Aharonov, Itai Arad, and Thomas Vidick. “Guest Column: The Quantum PCP Conjecture”. *SIGACT News* **44**, 47–79 (2013).
- [9] Barbara M. Terhal and David P. DiVincenzo. “Problem of equilibration and the computation of correlation functions on a quantum computer”. *Phys. Rev. A* **61**, 022301 (2000).

- [10] Arnau Riera, Christian Gogolin, and Jens Eisert. “Thermalization in Nature and on a Quantum Computer”. *Phys. Rev. Lett.* **108**, 080402 (2012).
- [11] Ersen Bilgin and Sergio Boixo. “Preparing Thermal States of Quantum Systems by Dimension Reduction”. *Phys. Rev. Lett.* **105**, 170405 (2010).
- [12] Jingxiang Wu and Timothy H. Hsieh. “Variational Thermal Quantum Simulation via Thermofield Double States”. *Phys. Rev. Lett.* **123**, 220502 (2019).
- [13] Anirban N. Chowdhury, Guang Hao Low, and Nathan Wiebe. “A Variational Quantum Algorithm for Preparing Quantum Gibbs States” (2020).
- [14] Youle Wang, Guangxi Li, and Xin Wang. “Variational Quantum Gibbs State Preparation with a Truncated Taylor Series”. *Phys. Rev. Applied* **16**, 054035 (2021).
- [15] Ada Warren, Linghua Zhu, Nicholas J. Mayhall, Edwin Barnes, and Sophia E. Economou. “Adaptive variational algorithms for quantum Gibbs state preparation” (2022).
- [16] Jonathan Foldager, Arthur Pesah, and Lars Kai Hansen. “Noise-assisted variational quantum thermalization”. *Scientific Reports* **12**, 3862 (2022).
- [17] D. Zhu, S. Johri, N. M. Linke, K. A. Landsman, C. Huerta Alderete, N. H. Nguyen, A. Y. Matsuura, T. H. Hsieh, and C. Monroe. “Generation of thermofield double states and critical ground states with a quantum computer”. *Proceedings of the National Academy of Sciences* **117**, 25402–25406 (2020).
- [18] Shavindra P. Premaratne and A. Y. Matsuura. “Engineering a Cost Function for Real-world Implementation of a Variational Quantum Algorithm”. In 2020 IEEE International Conference on Quantum Computing and Engineering (QCE). Pages 278–285. (2020).
- [19] R. Sagastizabal, S. P. Premaratne, B. A. Klaver, M. A. Rol, V. Negîrneac, M. S. Moreira, X. Zou, S. Johri, N. Muthusubramanian, M. Beekman, C. Zachariadis, V. P. Ostroukh, N. Haider, A. Bruno, A. Y. Matsuura, and L. DiCarlo. “Variational preparation of finite-temperature states on a quantum computer”. *npj Quantum Information* **7**, 1–21 (2021).
- [20] Troy J. Sewell, Christopher David White, and Brian Swingle. “Thermal Multi-scale Entanglement Renormalization Ansatz for Variational Gibbs State Preparation” (2022).
- [21] John Martyn and Brian Swingle. “Product spectrum ansatz and the simplicity of thermal states”. *Phys. Rev. A* **100**, 032107 (2019).
- [22] F. Verstraete, J. J. García-Ripoll, and J. I. Cirac. “Matrix Product Density Operators: Simulation of Finite-Temperature and Dissipative Systems”. *Phys. Rev. Lett.* **93**, 207204 (2004).
- [23] Anirban Narayan Chowdhury and Rolando D. Somma. “Quantum algorithms for Gibbs sampling and hitting-time estimation” (2016).
- [24] Christa Zoufal, Aurélien Lucchi, and Stefan Woerner. “Variational quantum Boltzmann machines”. *Quantum Machine Intelligence* **3**, 7 (2021).
- [25] Julien Gacon, Christa Zoufal, Giuseppe Carleo, and Stefan Woerner. “Simultaneous Perturbation Stochastic Approximation of the Quantum Fisher Information”. *Quantum* **5**, 567 (2021).
- [26] Xiaoyang Wang, Xu Feng, Tobias Hartung, Karl Jansen, and Paolo Stornati. “Critical behavior of Ising model by preparing thermal state on quantum computer” (2023).
- [27] Xiao Yuan, Suguru Endo, Qi Zhao, Ying Li, and Simon C. Benjamin. “Theory of variational quantum simulation”. *Quantum* **3**, 191 (2019).
- [28] Tobias Haug and Kishor Bharti. “Generalized quantum assisted simulator”. *Quantum Science and Technology* **7**, 045019 (2022).
- [29] K. Temme, T. J. Osborne, K. G. Vollbrecht, D. Poulin, and F. Verstraete. “Quantum Metropolis sampling”. *Nature* **471**, 87–90 (2011).
- [30] Man-Hong Yung and Alán Aspuru-Guzik. “A quantum–quantum Metropolis algorithm”. *Proceedings of the National Academy of Sciences* **109**, 754–759 (2012).
- [31] Mario Motta, Chong Sun, Adrian T. K. Tan, Matthew J. O’Rourke, Erika Ye, Austin J. Minnich, Fernando G. S. L. Brandão, and Garnet Kin-Lic Chan. “Determining eigenstates and thermal states on a quantum computer using quantum imaginary time evolution”. *Nature Physics* **16**, 205–210 (2020).
- [32] Oles Shtanko and Ramis Movassagh. “Algorithms for Gibbs state preparation on noiseless and noisy random quantum circuits” (2021).
- [33] Patrick Rall, Chunhao Wang, and Pawel Wocjan. “Thermal State Preparation via Rounding Promises” (2022).
- [34] Zoe Holmes, Gopikrishnan Muraleedharan, Rolando D. Somma, Yigit Subasi, and Burak Şahinoğlu. “Quantum algorithms from fluctuation theorems: Thermal-state preparation”. *Quantum* **6**, 825 (2022).
- [35] Luuk Coopmans, Yuta Kikuchi, and Marcello Benedetti. “Predicting Gibbs State Expectation Values with Pure Thermal Shadows” (2022).
- [36] João C. Getelina, Niladri Gomes, Thomas Iadecola, Peter P. Orth, and Yong-Xin Yao. “Adaptive variational quantum minimally entangled typical thermal states for finite temperature simulations” (2023).
- [37] Ingemar Bengtsson and Karol Zyczkowski. “Geometry of Quantum States: An Introduction to Quantum Entanglement”. Cambridge University Press. (2006).

- [38] Taku Matsui. “Purification and uniqueness of quantum Gibbs states”. *Communications in Mathematical Physics* **162**, 321–332 (1994).
- [39] Fabio Franchini. “An Introduction to Integrable Techniques for One-Dimensional Quantum Systems”. *Volume 940 of Lecture Notes in Physics*. Springer International Publishing. Cham (2017). [arXiv:1609.02100](https://arxiv.org/abs/1609.02100).
- [40] Armin Uhlmann. “Transition Probability (Fidelity) and Its Relatives”. *Foundations of Physics* **41**, 288–298 (2011).
- [41] Michael A. Nielsen and Isaac L. Chuang. “Quantum Computation and Quantum Information: 10th Anniversary Edition”. *Cambridge University Press*. (2010).
- [42] V. Vedral. “The role of relative entropy in quantum information theory”. *Rev. Mod. Phys.* **74**, 197–234 (2002).
- [43] Jorge Nocedal and Stephen J. Wright. “Numerical Optimization”. *Springer*. New York, NY, USA (2006). 2e edition.
- [44] IBM Quantum. “Compute resources”. <https://quantum-computing.ibm.com/services/resources> (2022).
- [45] Gushu Li, Yufei Ding, and Yuan Xie. “Tackling the Qubit Mapping Problem for NISQ-Era Quantum Devices” (2018).
- [46] J.C. Spall. “Multivariate stochastic approximation using a simultaneous perturbation gradient approximation”. *IEEE Transactions on Automatic Control* **37**, 332–341 (1992).
- [47] Paul D. Nation, Hwajung Kang, Neereja Sundaresan, and Jay M. Gambetta. “Scalable Mitigation of Measurement Errors on Quantum Computers”. *PRX Quantum* **2**, 040326 (2021).
- [48] Antonio Sanna, Andrea Giordano, Nicola Lo Gullo, Carlo Mastroianni, and Francesco Plastina. “A hybrid classical-quantum approach to speed-up Q-learning”. *Scientific Reports* **13**, 3913 (2023).
- [49] Yasunari Suzuki, Yoshiaki Kawase, Yuya Masumura, Yuria Hiraga, Masahiro Nakadai, Jibao Chen, Ken M. Nakanishi, Kosuke Mitarai, Ryosuke Imai, Shiro Tamiya, Takahiro Yamamoto, Tennin Yan, Toru Kawakubo, Yuya O. Nakagawa, Yohei Ibe, Youyuan Zhang, Hirotsugu Yamashita, Hikaru Yoshimura, Akihiro Hayashi, and Keisuke Fujii. “Qulacs: A fast and versatile quantum circuit simulator for research purpose”. *Quantum* **5**, 559 (2021).
- [50] Qiskit contributors. “Qiskit: An Open-source Framework for Quantum Computing”. <https://quantum-computing.ibm.com> (2023).
- [51] Mirko Consiglio. “Variational Gibbs State Preparation”. <https://github.com/mirkoconsiglio/VariationalGibbsStatePreparation> (2023).

A Error Analysis of Measurements

In this Appendix, we perform an analysis of the error scaling with the number of shots, in faithfully identifying the probability distribution, $\vec{p} = \{p_0, p_1, \dots, p_{d-1}\}$, where $d = 2^n$, prepared by U_A . The outcome of one shot of a quantum circuit can be described by a multinomial distribution, where p_i is the probability of observing a bit string i . The expected value of a multinomially distributed random bit string i is

$$\mu = \mathbb{E}[i] = np_i, \quad (19)$$

with the variance being

$$\sigma^2 = \text{Var}[i] = np_i(1 - p_i). \quad (20)$$

A quantity that can describe the precision of measuring the bit string i , p_i times, is the coefficient of variation, or relative standard deviation,

$$c_v = \frac{\sigma}{\mu} = \sqrt{\frac{1 - p_i}{N_s p_i}}. \quad (21)$$

Given that $p_i = \exp(-\beta E_i)/\mathcal{Z}_\beta$ for the Boltzmann distribution, we get

$$c_v = \sqrt{\frac{1 - \frac{e^{-\beta E_i}}{\mathcal{Z}_\beta}}{N_s \frac{e^{-\beta E_i}}{\mathcal{Z}_\beta}}} = \sqrt{\frac{\mathcal{Z}_\beta - e^{-\beta E_i}}{N_s e^{-\beta E_i}}} = \sqrt{\frac{1}{N_s} \left(\frac{\mathcal{Z}_\beta}{e^{-\beta E_i}} - 1 \right)}. \quad (22)$$

From Eq. (22), if $\beta \rightarrow 0$, then $\mathcal{Z}_\beta / \exp(-\beta E_i) \rightarrow d \forall i \in [d]$, which implies

$$c_v(\beta \rightarrow 0) = \sqrt{\frac{d - 1}{N_s}}, \quad (23)$$

hence, exhibiting an exponential scaling in the number of shots needed for preparing the flat distribution. On the other hand, if $\beta \rightarrow \infty$, then $\mathcal{Z}_\beta / \exp(-\beta E_0) \rightarrow 1$, while all other probabilities tend to zero, and the algorithm reduces to finding the ground-state of the Hamiltonian. As a result,

$$c_v(\beta \rightarrow \infty) = 0. \quad (24)$$

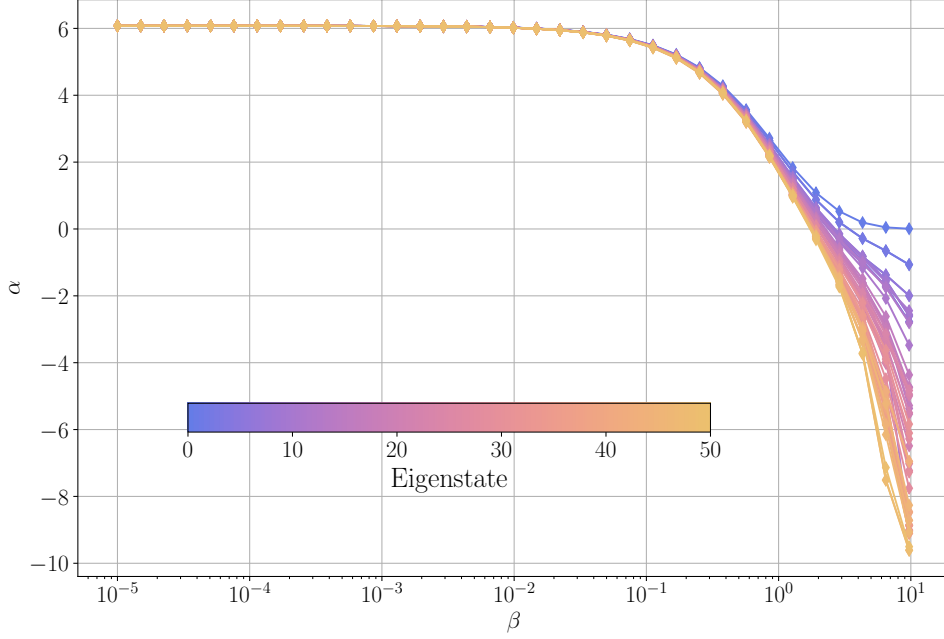


Figure 8: The exponent α_i in Eq. (25) is plotted vs β for the first 51 p_i , where each point is the polynomial fit for n between 8 and 20.

For intermediary temperatures, we carry out a qualitative analysis. Fig. 8 reports the exponent α_i , of a polynomial fit of the normalized coefficient of variation, defined as

$$c_v \sqrt{N_s} = C n^{\alpha_i}, \quad (25)$$

for n between 8 and 20, at different β , where the first 51 p_i of the Ising model with $h = 0.5$ are considered. We see that as $\beta \rightarrow \infty$, the exponent α_0 goes to zero only for the ground-state occupation probability p_0 , in accordance with Eq. (24), and as the occupation probability p_i of an excited state becomes vanishingly small, the respective exponent α_i becomes increasingly negative. On the other hand, for any finite temperature, we see that a polynomial fit, with $\alpha_i \in [0, 6.0768]$, approximates well the normalized coefficient of variation. This implies that a sub-exponential scaling of shots is required to obtain a faithful reconstruction of the probability distribution, for the system sizes of the Ising model investigated in NISQ algorithms, as done in the main text of the manuscript.

B Necessity of Entangling Gates in U_A

In the main text, we specified that we required entanglement in the ancillary register to be able to faithfully prepare the Boltzmann distribution of the Ising model. While we only used one layer of a hardware-efficient ansatz, we concluded that this was sufficient to approximate the Boltzmann distribution with a high fidelity for the system sizes we investigated. However, at least one entangling layer is necessary for preparing the Boltzmann distribution of the Ising model, and we will show this by considering the converse. Suppose the ancilla ansatz is a single layer of local R_Y gates, then we get

$$\begin{aligned} \bigotimes_{i=0}^{n-1} R_Y(\theta_i) |0\rangle_i &= \bigotimes_{i=0}^{n-1} \left(\cos\left(\frac{\theta_i}{2}\right) |0\rangle_i + \sin\left(\frac{\theta_i}{2}\right) |1\rangle_i \right) \\ &= \sum_{i=0}^{d-1} \prod_{j \in S_{i=0}} \cos\left(\frac{\theta_j}{2}\right) \prod_{k \in S_{i=1}} \sin\left(\frac{\theta_k}{2}\right) |i\rangle \\ &= \sum_{i=0}^{d-1} p_i |i\rangle, \end{aligned} \quad (26)$$

where $S_{i=0} \equiv \{j \mid j = 0 \forall \text{ bits } j \in i\}$, that is, the set of bits in i which are equal to 0, and similarly defined for $S_{i=1}$, and $|i\rangle$ is the computational basis state. This implies that

$$\prod_{j \in S_{i=0}} \cos\left(\frac{\theta_j}{2}\right) \prod_{k \in S_{i=1}} \sin\left(\frac{\theta_k}{2}\right) = p_i. \quad (27)$$

Now, without loss of generality, consider these specific cases:

$$\prod_{j=0}^{n-1} \cos\left(\frac{\theta_j}{2}\right) = p_0, \quad (28a)$$

$$\prod_{j=0}^{n-2} \cos\left(\frac{\theta_j}{2}\right) \sin\left(\frac{\theta_{n-1}}{2}\right) = p_1, \quad (28b)$$

$$\prod_{j=0}^{n-3} \cos\left(\frac{\theta_j}{2}\right) \cos\left(\frac{\theta_{n-1}}{2}\right) \sin\left(\frac{\theta_{n-2}}{2}\right) = p_2, \quad (28c)$$

$$\prod_{j=0}^{n-3} \cos\left(\frac{\theta_j}{2}\right) \sin\left(\frac{\theta_{n-2}}{2}\right) \sin\left(\frac{\theta_{n-1}}{2}\right) = p_3. \quad (28d)$$

Combining the above equations results in

$$\frac{p_0}{p_1} = \frac{\cos\left(\frac{\theta_{n-1}}{2}\right)}{\sin\left(\frac{\theta_{n-1}}{2}\right)}, \quad (29a)$$

$$\frac{p_0}{p_2} = \frac{\cos\left(\frac{\theta_{n-2}}{2}\right)}{\sin\left(\frac{\theta_{n-2}}{2}\right)}, \quad (29b)$$

$$\frac{p_0}{p_3} = \frac{\cos\left(\frac{\theta_{n-2}}{2}\right) \cos\left(\frac{\theta_{n-1}}{2}\right)}{\sin\left(\frac{\theta_{n-2}}{2}\right) \sin\left(\frac{\theta_{n-1}}{2}\right)}, \quad (29c)$$

and finally, combining the above equations implies that

$$\begin{aligned} \frac{p_0}{p_1} \frac{p_0}{p_2} &= \frac{p_0}{p_3} \implies \frac{p_0}{p_1 p_2} = \frac{1}{p_3} \\ &\implies p_0 p_3 = p_1 p_2 \\ &\implies e^{-\beta E_0} e^{-\beta E_3} = e^{-\beta E_1} e^{-\beta E_2}. \end{aligned} \quad (30)$$

Applying logs to both sides and simplifying, we get

$$E_0 + E_3 = E_1 + E_2, \quad (31)$$

which is not in general true for the Ising model. The above reasoning can be adjusted to obtain further constraints in the manner of Eq. (31).